RAPID COMMUNICATIONS

PHYSICAL REVIEW B VOLUME 52, NUMBER 12 15 SEPTEMBER 1995-II

General picture of quantum Hall transitions in quantum antidots

D. R. Mace and C. H. W. Barnes
Cavendish Laboratory, Madingley Road, Cambridge CB3 0HE, United Kingdom

G. Faini and D. Mailly
Laboratoire de Microstructures et de Microelectronique - CNRS, 196, Avenue Henri Ravera, 92220 Bagneux, France

M. Y. Simmons, C. J. B. Ford, and M. Pepper
Cavendish Laboratory, Madingley Road, Cambridge CB3 0HE, United Kingdom
(Received 9 May 1995)

In this paper we present a general picture of the cyclic change in resonant structure seen in conductance across quantum Hall transitions in quantum antidots. The cycle begins with resonant dips below the ne^2/h plateau, which evolve into resonant peaks above it. A sinusoidal oscillation, of shorter period in magnetic field, then appears, which evolves into resonant dips below the $(n+1)e^2/h$ plateau. The cycle repeats for successive transitions. We provide an explanation for this behavior in terms of the edge-state model and show by numerical calculation that this picture accounts in detail for the line shapes and dependencies observed experimentally.

The existence of the quantum Hall effect[1] in highly disordered silicon metal-oxide-semiconductor field-effect transistors indicated a fundamental simplicity in the nature of electronic transport in these complex systems. The underlying reason for this quantization was shown to be the division of the wave function at the Fermi energy (E_F) into spatially separated edge states that follow equipotentials in the two-dimensional electron gas (2DEG).[2,3] In a large device the transition regions between quantum Hall (QH) plateaus are smooth; however, in smaller devices, at milli-Kelvin temperatures, a complex pattern of resonant structure is resolved that may be associated with communication across the 2DEG via localized edge states that form around closed equipotentials. At the high-magnetic-field end of a QH transition this structure typically consists of conductance peaks that may be associated with resonant transmission through states trapped in cavities: quantum dots (QD's).[4] At the low-field end, conductance dips are typically observed; these may be associated with resonant reflection via localized states magnetically bound to peaks: quantum antidots (QAD's).[5,6] However, at a general point in a QH transition the presence of more than one Landau level (LL), and thus the possibility for inter-LL scattering, can produce resonant reflection from QD's and resonant transmission through QAD's.[7] Variations in both the scattering strengths, and the occupation of bound states of different LL's around single QAD's or QD's leads, in general, to the conductance across a QH transition being a complex pattern of peaks and dips with asymmetric and non-Lorentzian line shapes. In this paper we make a detailed experimental and theoretical investigation of these conductance patterns in a single QAD, and propose a cyclic pattern in this structure across any QH transition. Our aim is to provide a comprehensive understanding of such transitions, which may be used as a basis for distinguishing between the different contemporary theories of edge states.[2,8–13]

The paper is organized as follows: we first present our experimental QAD with the corresponding edge-state scattering picture. We then describe the changes in scattering, and the resulting effect on the resonant conductance profiles, across any QH transition with reference to the $\nu=2$ to $\nu=4$ transition (ν is the LL filling factor), and present detailed experimental conductance data for this transition. Finally, we make a quantitative comparison between our data and a numerical evaluation of the expected scattering diagram.

Our experimental QAD is defined using an independently contacted gate placed in the center of a split gate (SG) to form two parallel ballistic constrictions.[14,15] The QAD lithographic diameter is 0.2 μm, the SG lengths are 0.3 μm, and the separation between the side gates and the QAD is 0.3 μm. The device was fabricated on a $GaAs/Al_xGa_{1-x}As$ heterostructure with the 2DEG 100 nm below the surface, carrier density 3.3×10^{15} m^{-2}, and mobility 60 m^2 V^{-1} s^{-1} after brief illumination. The device was measured at temperatures below 100 mK using low-voltage and low-frequency ac techniques in a magnetic field such that the minimum filling factor $\nu=7$ in the bulk. The gate voltages were set so that the SG widths were as closely matched as possible. Three important factors make this the ideal regime in which to study the general features of a QH transition: (1) Both inter- and intra-LL scattering are present. (2) E_F in the bulk is approximately independent of magnetic field. (3) The absence of spin-flip scattering allows us to treat the QAD conductance as the sum of those for spin up and spin down, $G=G\uparrow+G\downarrow$.

Within linear response theory at low temperature, the wave function at E_F determines the conductance of a quantum system. In a magnetic field this wave function may be constructed as a superposition of edge states. The conductance of a network of edge states may be calculated within the Landauer-Büttiker formalism with unitary scattering probabilities between any pair of edge states that are sufficiently close.[16] In a transition where the $(n+1)$th LL changes from being perfectly reflected to perfectly transmit-

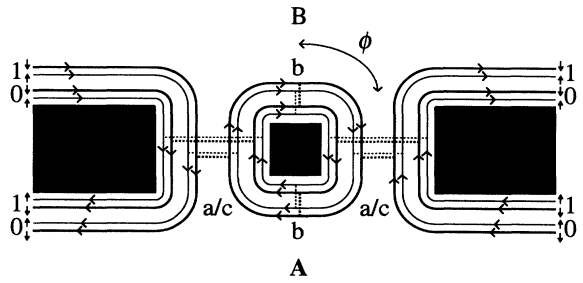

FIG. 1. A schematic diagram of the QAD. Edge states are represented as solid lines, the scattering events relevant to this paper are shown as dashed lines.

ted through a QAD, we might expect scattering in the nth and $(n+1)$th LL's to dominate the conductance, since contributions from other LL's are exponentially smaller. This assumption allows us to discuss a general QH transition in terms of the simplest case, which is the transition involving the $n=0$ and $n=1$ LL's. At low magnetic fields approximate spin degeneracy causes this transition to consist of two separate transitions that occur simultaneously, i.e., the $\nu=2$ to $\nu=4$ QH transition. Figure 1 gives the edge-state scattering mechanism for this transition. It does not include spin-flip scattering. Events a and c are intraedge-state scattering for the $n=0$ and $n=1$ LL's, respectively; b is interedge-state scattering between the $n=0$ and $n=1$ LL's. They occur with probabilities p_a^2, p_b^2, and p_c^2. Interedge-state scattering probabilities from higher LL's are much smaller since these states lie further from the QAD.

In our device, a QH transition ν to $\nu+2$ may be induced by either a reduction in magnetic field B or a reduction in the magnitude of the center gate voltage V_g. To understand the B and V_g dependence of the scattering probabilities we must bear in mind two points: (1) When edge states move further apart their physical overlap reduces and the corresponding scattering probabilities reduce. (2) In a magnetic field states lie at energies $\approx(n+\frac{1}{2})\hbar\omega_c \pm \frac{1}{2}g\mu_B B$ above the QAD potential. *Transition in B*: When we reduce B the edge states move closer to the potential walls and closer together and therefore $p_{a/c}^2$ decrease and p_b^2 increases on average. In detail, p_b^2 may increase or decrease depending on the precise shape of the QAD potential. Also, if b represents more than one scattering event, p_b^2 may oscillate with the beat frequency between the two LL's.[17] *Transition in* V_g: When we reduce V_g both the radius (R) and the gradient (E_g) of the QAD potential at E_F are reduced. When R is reduced the constriction widths increase and $p_{a/c}^2$ decrease but p_b^2 does not change. As E_g is decreased the states encircling the QAD move outwards and apart; p_b^2 decreases and $p_{a/c}^2$ increase. In addition, spin splitting causes $p_{a/c\uparrow}^2$ to be less than $p_{a/c\downarrow}^2$ but $p_{b\uparrow}^2 \approx p_{b\downarrow}^2$.

The closed edge states encircling the QAD form a set of bound states which may be swept through E_F as a function of V_g or B. The conductance of the QAD, measured between points A and B in Fig. 1, shows resonant structure when one of these states passes E_F. The nature of the resonance is a sensitive function of the probabilities p_a^2, p_b^2, and p_c^2. When $p_c^2=1$ and $p_a^2>(<)p_b^2/(1+p_b^2)$ resonant dips (peaks) below (above) the $2e^2/h$ plateau occur due to bound states of the $n=0$ LL. Naively one might expect the condition to be $p_c^2=1$ and $p_a^2>(<)p_b^2$; however, the asymmetry arises due to the absence of time-reversal symmetry. When $p_c^2<1$ a second set of bound states in the $n=1$ LL forms, giving rise to a second set of resonances. These states enclose a larger area than those of the $n=0$ LL and so the resonances have a shorter period as a function of B.

In a general QH transition, this picture predicts that resonant dips below the ne^2/h plateau, due to intraedge-state scattering through the nth LL bound states, evolve into resonant peaks as interedge-state scattering between the $(n+1)$th LL and nth LL becomes dominant. When bound states of the $(n+1)$th LL begin to form, a sinusoidal modulation of the conductance appears, and as the $(n+1)e^2/h$ plateau is approached the modulations evolve into resonant dips below this plateau, thus completing the cycle.

We are now in a position to understand our complex experimental data. Figure 2(a) shows a series of B sweeps, which illustrates the first part of our cycle. Sweep 1, at greatest V_g, shows alternating pairs of resonant dips down below $2e^2/h$. Successive dips, from different spins, have different

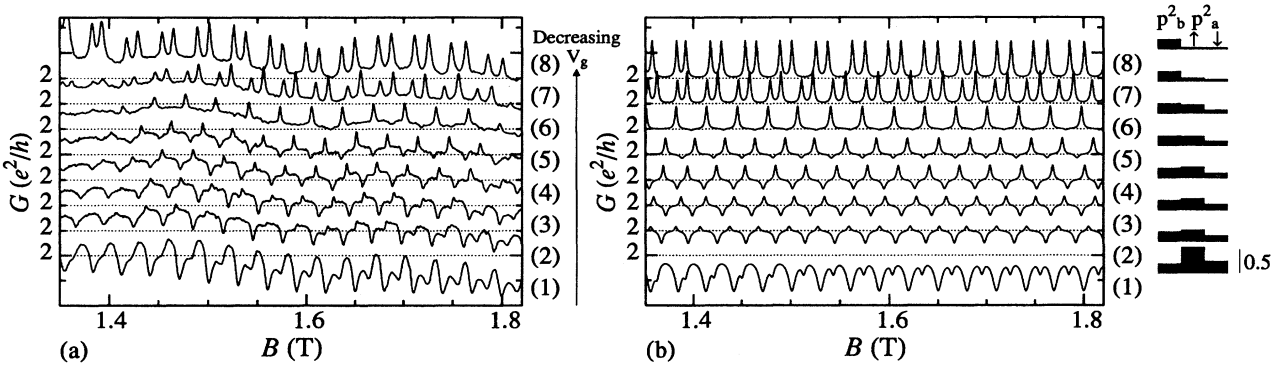

FIG. 2. Conductance of the QAD at decreasing V_g illustrating part of our hierarchy: (a) Experimental data in the regime where decreasing intraedge-state scattering in the $n=0$ LL becomes dominated by interedge-state scattering, and (b) the conductance curves and scattering probabilities obtained from our model. The vertical offset between curves is e^2/h.

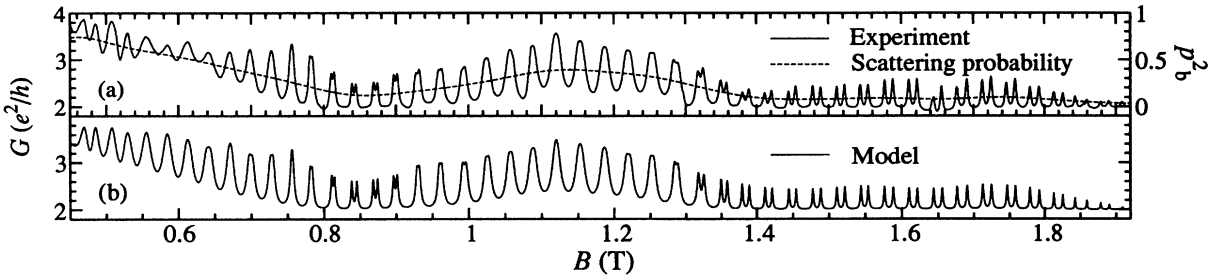

FIG. 3. (a) The solid line is experimental data, dominated by interedge-state scattering only. The dashed line shows the calculation of p_b^2. (b) Similar oscillations are produced by the model using these values of $p_b^2(B)$ with a small constant p_a^2.

amplitudes since $p_{a\uparrow}^2 < p_{a\downarrow}^2$. In subsequent sweeps, as we reduce V_g, p_a^2 decreases whereas p_b^2 remains roughly constant. The conductance on resonance increases in magnitude and the dips gradually become peaks, first for one spin, and then the other. At the smallest V_g, pairs of peaks with equal heights occur showing that p_a^2 has become exponentially small and $p_{b\uparrow}^2 = p_{b\downarrow}^2$.

Figure 3(a) shows data, similar to that of sweep 8, Fig. 2(a), in which the conductance is dominated by interedge-state scattering. Over this large field range we expect p_b^2 to decrease on average. We have made an estimate of p_b^2 as a function of B, shown as a dashed line. (This calculation is discussed later.) The nonmonotonic decrease in p_b^2, with a minimum at 0.85 T, gives rise to the illusion that the spin splitting has a maximum at 0.85 T. It does not. As p_b^2 increases either side of 0.85 T, the width of the peaks increases, due to the reduced confinement, so that the spin splitting can no longer be resolved.

Figure 4(a) shows the variation of conductance as we continue to reduce V_g. (Sweep 1 is a section from Fig. 3.) As intraedge-state scattering in the $n=1$ LL becomes significant ($p_c^2 < 1$) the corresponding bound states form. This gives rise to a sinusoidal oscillation of shorter period appearing in addition to the interedge-state scattering peaks. This is clearest in the center of the figure (sweep 6) where the two oscillations are out of phase and p_b^2 is a minimum. On either side of the graph the broad oscillations due to the greater p_b^2 combine with the sinusoidal oscillation to produce asymmetric line shapes. The peak width of the sinusoidal oscillation decreases as V_g is reduced, and sweeps 7 and 8 show the predicted dips down from the $4e^2/h$ plateau between 0.8 T and 0.9 T. Sweep 8 also shows peaks above $4e^2/h$, due to interedge-state scattering between the $n=2$ and $n=1$ LL's. This is the start of the $\nu=4$ to $\nu=6$ transition as expected from the cycle of resonant behavior we have proposed.

We have described the qualitative behavior expected from the simple edge-state picture, but a deeper comparison can be made by evaluating the conductance predicted by the diagram in Fig. 1:[16] The conductance $G = 2 - Tr(\mathbf{TT}^\dagger)$ for each spin where $\mathbf{T} = \mathbf{T}_{a/c}\mathbf{T}_b(\mathbf{1} - \mathbf{BT}_b^\dagger\mathbf{AT}_b)^{-1}\mathbf{T}_{a/c}$ and

$$\mathbf{A} = \begin{bmatrix} 0 & \lambda_4\lambda_2^* r_a \\ \lambda_3\lambda_1^* r_c & 0 \end{bmatrix}, \quad \mathbf{B} = \begin{bmatrix} 0 & \lambda_1 r_c \\ \lambda_2 r_a & 0 \end{bmatrix},$$

$$\mathbf{T}_{a/c} = \begin{bmatrix} t_c & 0 \\ 0 & t_a \end{bmatrix}, \quad \mathbf{T}_a = \begin{bmatrix} t_b & r_b \\ r_b & t_b \end{bmatrix},$$

with $\lambda_1 = \exp(2il_0\phi)$, $\lambda_2 = \exp(2il_1\phi)$, $\lambda_3 = \exp(2il_0\pi)$, and $\lambda_4 = \exp(2il_1\pi)$. The r's and t's are the reflection and transmission coefficients of the scattering events a, b, and c. We choose the scattering phase shifts such that $r = \sqrt{1-p^2}$ and $t = ip$. ϕ is the angle between scattering events b and a. The conductance G exhibits a resonance whenever l_0 or l_1 become integers.

We use this model to test quantitatively the relationships between p_a^2, p_b^2, and p_c^2 and the conductance, and we calcu-

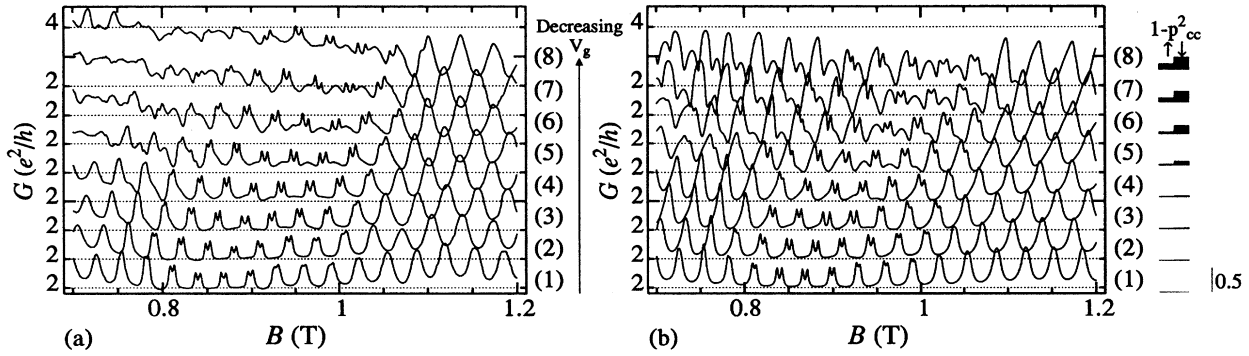

FIG. 4. The effect of the onset of intraedge-state scattering in the $n=1$ LL: (a) Experimental data, and (b) the conductance obtained from the model with the associated scattering probabilities (for clarity $1-p_{cc}^2$ is shown). The vertical offset between curves is $2e^2/h$.

late p_a^2, p_b^2, and p_c^2 from the experimental data. We can assume that symmetric scattering probabilities are equal since in the experiment the SG's were adjusted to be identical. We have not, as yet, discussed the positions of the resonances in B and V_g; such a discussion is necessarily very involved and in the case of QD's has provoked considerable debate over many years.[4] These positions are also subject to the influence of the Coulomb blockade.[18] The positions form part of the input for our model in the form of the dependencies of l_0 and l_1. For our purposes it is not necessary to calculate these positions numerically from the QAD many-particle addition spectrum since it is sufficient to take them from the experiment.

Figure 2(b) shows the model predictions for the conductance sweeps in Fig. 2(a) with our estimates of the scattering probabilities. For each sweep all scattering probabilities are constant. Since all sweeps were taken over a small V_g range, p_b^2 is constant throughout. The high magnetic field implies $p_c^2=1$ for all sweeps, and thus ϕ plays no part in the conductance. Successive sweeps are distinguished by having reduced p_a^2.

Figure 3(b) shows the prediction for the conductance sweep in Fig. 3(a). $p_a^2(=0.05)$ is constant throughout; it may be estimated from the peak heights following the analysis of Fig. 2(a). $p_c^2=1$ and p_b^2 is a function of B. Under these conditions the convolution of G with the derivative of the Fermi function, at a sufficiently high temperature, is a function of p_b^2 only; we make the corresponding convolution of the experimental data to determine $p_b^2(B)$.

Figure 4(b) shows the predictions for the conductance sweeps in Fig. 4(a). $p_a^2=0.05$ for all sweeps. $p_b^2(B)$ is known for sweep 1 since it is a section from Fig. 3; the same procedure may not be used to calculate $p_b^2(B)$ for subsequent sweeps as $p_c^2<1$. As V_g is varied the potential features that give rise to a specific $p_b^2(B)$ move and hence $p_b^2(B)$ is different for each sweep. However, over a sufficiently small range of V_g we expect this change to be linear and therefore we can write $p_{b(s+1)}^2(B)=p_{b(s)}^2(B-\Delta B)$ for sweeps s and $s+1$. $\Delta B=13$ mT, deduced from the data which shows a clear shift in the minimum of $p_b^2(B)$. p_c^2 increases with increasing magnetic field. From the amplitude of the sinusoidal oscillations, we calculate the value of p_c^2 at the center of each sweep (p_{cc}^2), where the two oscillations are clearest. As V_g is reduced, E_g decreases, and the B dependence of p_c^2 becomes stronger. Over a small range in B we may write $p_c^2 \propto(1-p_{cc}^2)B$. The values of p_{cc}^2 are shown in the figure.

The quality of agreement between our experiment and model justifies our statement that interedge-state scattering from higher LL's is not important. Sweeps 5–8, for fields below 0.85 T, show the beginning of the next cycle where intraedge-state scattering in the $n=1$ LL and interedge-state scattering between the $n=2$ and $n=1$ LL's become significant. The latter results in the experimental dips down from $4e^2/h$ being less deep than those predicted, and when dominant, gives peaks above $4e^2/h$ as shown in sweep 8. In this regime, interedge-state scattering between the $n=2$, $n=1$, and $n=0$ LL's may occur. If interedge-state scattering to lower LL's is sufficiently strong, oscillations with periods relating to every possible closed-loop path in the edge-state scattering diagram will superimpose, giving very complex structure consistent with our cycle.

In conclusion, we have presented a general picture of cyclic change in resonant structure seen in conductance across quantum Hall transitions in QAD's which is directly attributable to a pattern of changing scattering probabilities between edge states. We have confirmed this cycle for the $\nu=2$ to $\nu=4$ transition; further confirmation is provided by numerical evaluation of the relevant scattering diagram.

We acknowledge C. Mayeux and D. Arquey for technical support and the UK EPSRC and ESPRIT Basic Research Action No. 6536 for financial support.

[1] K. von Klitzing, G. Dorda, and M. Pepper, Phys. Rev. Lett. **45**, 494 (1980).

[2] B. I. Halperin, Phys. Rev. B **25**, 2185 (1982); P. Streda, J. Kucera, and A. H. MacDonald, Phys. Rev. Lett. **59**, 1973 (1987); J. K. Jain and S. A. Kivelson, Phys. Rev. B **37**, 4276 (1988); M. Büttiker, *ibid.* **38**, 9375 (1988).

[3] C. W. J. Beenakker and H. van Houten, in *Solid State Physics*, edited by H. Ehrenreich and D. Turnbull (Academic, San Diego, 1991), Vol. 44, p. 1; M. Büttiker, in *Semiconductors and Semimetals*, edited by M. A. Reed (Academic, New York, 1992), Vol. 35, p. 191; S. E. Ulloa, A. MacKinnon, E. Castaño, and G. Kirczenow, in *Handbook on Semiconductors*, edited by P. T. Landsberg (North-Holland, Amsterdam, 1992).

[4] P. L. McEuen *et al.*, Phys. Rev. B **45**, 11 419 (1992); R. C. Ashoori *et al.*, Phys. Rev. Lett. **68**, 3088 (1992); P. L. McEuen *et al.*, Physica B **189**, 70 (1993).

[5] J. K. Jain and S. A. Kivelson, Phys. Rev. Lett. **60**, 1542 (1988); J. K. Jain, *ibid.* **60**, 2074 (1988).

[6] G. Timp *et al.*, Phys. Rev. Lett. **58**, 2814 (1987); P. H. M. Loosdrecht *et al.*, Phys. Rev. B **38**, 10 162 (1988); J. A. Simmons *et al.*, Phys. Rev. Lett. **63**, 1731 (1989); R. Mottahedeh *et al.*, Solid State Commun. **72**, 1065 (1989).

[7] R. P. Taylor *et al.*, Surf. Sci. **263**, 247 (1992); Phys. Rev. Lett. **69**, 1989 (1992); A. S. Sachrajda *et al.*, Phys. Rev. B **47**, 6811 (1993).

[8] A. M. Chang, Solid State Commun. **74**, 871 (1990).

[9] D. B. Chklovskii, B. I. Shklovskii, and L. I. Glazman, Phys. Rev. B **46**, 4026 (1992).

[10] K. Leir and R. R. Gerhardts, Phys. Rev. B **50**, 7757 (1994).

[11] X. G. Wen, Phys. Rev. Lett. **64**, 220 (1990); Phys. Rev. B **43**, 11 025 (1991); **44**, 5608 (1991).

[12] C. L. Kane *et al.*, Phys. Rev. Lett. **72**, 4129 (1994).

[13] George Kirczenow and Brad L. Johnson, Phys. Rev. B **51**, 17 579 (1995).

[14] P. J. Simpson *et al.*, Appl. Phys. Lett. **63**, 3191 (1993).

[15] R. P. Taylor *et al.*, J. Vac. Sci. Technol. B **11**, 628 (1993).

[16] G. Kirczenow, Phys. Rev. B **50**, 1649 (1994).

[17] G. Kirczenow *et al.*, Phys. Rev. Lett. **72**, 2069 (1994).

[18] C. J. B. Ford *et al.*, Phys. Rev. B **49**, 17 456 (1994).